79-4035

Fatigue Failure of Multidirectional Laminate

Assa Rotem*
Technion—Israel Institute of Technology, Haifa, Israel

A general fatigue failure criterion for laminates made of unidirectional laminae in different directions is evolved, based on previously developed concepts. A limited number of fatigue functions are measured from tests on single lamina and one type of angle-ply laminate. The fatigue functions used in the fatigue failure criterion enable prediction of the fatigue life of any laminate. An extensive tension-tension fatigue testing program for E-glass/epoxy symmetric-balanced laminates with various reinforcement angles has been carried out in order to test the validity of the theory. The test results were in good agreement with the predicted fatigue failure mode relevant to the specific laminate. In some cases there is shifting from one failure mode to another due to the progressive nature of the fatigue failure.

Nomenclature

A,B,D	= stiffness matrices
b	= half-width of the laminate
c	= cycles/unit time
E_A,E_T,G_A,ν_A	= engineering elastic constants of lamina
f	= fatigue function
G	= shear modulus of the interlaminar layer
h	= distance from the midplane of a laminate
K	= constant value in the expression for interlaminar shear
M	= moment for unit length
n	= number of cycles
N	= number of cycles to failure
P	= force for unit length
Q_{ij}	= elastic constants of a lamina (i = 1,2,6)
R	= stress ratio
S_{xx}	= compliance
t	= thickness of a lamina
t_i	= thickness of interlaminar layer
t_ℓ	= thickness of a laminate
Z	= coordinate perpendicular to the laminate plane
σ_{ij}	= general state of stress
σ	= normal stress
τ	= shear stress
ϵ	= strain
ϵ_0	= strain in the midplane
κ	= curvature
ρ_I,μ,η,k_{ij}	= expressions
θ	= angle

Subscripts

x	= x direction
A	= fiber direction
d	= interlaminar
T	= transverse to fiber direction
τ	= a shear
p	= a lamina
ℓ	= a laminate
m	= a matrix

Superscripts

u	= fatigue failure
s	= static failure
c	= cyclic load

Received Dec. 28, 1977; revision received Oct. 2, 1978.

Index categories: Structural Composite Materials; Structural Durability (including Fatigue and Fracture).

*Associated Professor, Faculty of Mechanical Engineering, Material Mechanics Laboratory.

Introduction

In a previous article,[1] a fatigue failure criterion for unidirectional fiber-reinforced materials was developed and examined. This criterion was extended for angle-ply laminates[2] where the strain field is different from the case of the single lamina loaded in an off-axis direction. Nevertheless, when the angle-ply laminate is loaded in the direction of bisectors of reinforcement angles, all laminae in the laminate will be in an almost identical stress field, differing only in the direction of the shear stresses. Therefore, the in-plane failure might onset at any of the laminae simultaneously, and a noncumulative fatigue failure criterion is needed to predict such failure. In addition to the in-plane failure, delamination might start as a result of the interlaminar shear and/or tension stresses on the free boundaries. Such failure is expected for angle-ply laminates, where the angle of reinforcement causes the interlaminar shear and/or tension to be high enough to cause delamination before in-plane failure occurs.

In both cases, the fatigue failure criterion, namely the off-axis lamina and the angle-ply laminate (for in-plane failure), is based on two fatigue functions which can be determined experimentally. For fatigue failure of unidirectional lamina loaded in the fiber direction, we need an additional fatigue function; in the case of delamination, we need a further two fatigue functions.

A multidirectional laminate is far more complicated; as each lamina is under a different stress field, failure may occur at some lamina after a certain amount of load cycling while the other laminae are still far from failure. The laminate does not necessarily fail as a whole after the first lamina failure. The remaining lifetime, in terms of loading cycling, depends on the construction of the laminate. This research is concerned with this subject; namely, to find and examine a fatigue failure criterion for multidirectional laminate based on a few, experimentally determined fatigue functions.

Analytical

A uniaxially reinforced lamina in plane stress has two different failure modes, as shown in Ref. 1—one for fiber fracture, the other for matrix fracture. When an angle-ply laminate is produced from the uniaxial laminae, each lamina is still in plane stress condition, except at the vicinity of the free edge, as analytically[3-5] and experimentally,[6] shown in several articles. The same is true for a multidirectional laminate under in-plane loadings, but in contrast to the angle-ply laminate under symmetrical in-plane loading where the stress field in all laminae is essentially the same, in the multidirectional laminate different stress fields exist in the laminae which cause successive failure.

As shown in Ref. 1, the fiber fracture mode of fatigue failure can be expressed mathematically in the following manner:

$$\sigma_A^c \geqq \sigma_A^u \qquad (1)$$

with

$$\sigma_A^u = \sigma_A^s f_A(R,N,c) \qquad (2)$$

The matrix mode of the fatigue failure is expressed by:

$$(\sigma_T^c/\sigma_T^u)^2 + (\tau^c/\tau^u) \geqq 1 \qquad (3)$$

where

$$\sigma_T^u = \sigma_T^s f_T(R,N,c)$$

$$\tau^u = \tau^s f_\tau(R,N,c)$$

In the same manner, the interlaminar fatigue failure mode is expressed by:

$$(\sigma_d^c/\sigma_d^u)^2 + (\tau_d^c/\tau_d^u)^2 \geqq 1 \qquad (4)$$

with

$$\tau_d^u = \tau_d^s f_d(R,N,c)$$

$$\sigma_d^u = \sigma_d^s f_d'(R,N,c) \qquad (5)$$

Consider the case of a general multidirectional laminate under in-plane cyclic loading of forces and moments. Assuming elastic laminae, the load-strain relationship is expressed by the matrix equation[7]:

$$\begin{vmatrix} P^c \\ M^c \end{vmatrix} = \begin{vmatrix} A & B \\ B & D \end{vmatrix} \begin{vmatrix} \epsilon_0^c \\ \kappa^c \end{vmatrix} \qquad (6)$$

where $[A]$ $[B]$ and $[D]$ are the stiffness matrices expressed by:

$$A_{ij} = \sum_{p=1}^{n} {}_pQ_{ij}({}_ph - {}_{(p-1)}h) \qquad (7a)$$

$$B_{ij} = \frac{1}{2}\sum_{p=1}^{n} {}_pQ_{ij}({}_ph^2 - {}_{(p-1)}h^2) \qquad (7b)$$

$$D_{ij} = \frac{1}{3}\sum_{p=1}^{n} {}_pQ_{ij}({}_ph^3 - {}_{(p-1)}h^3) \qquad (7c)$$

and it is assumed that the stresses are constant through the thickness of each lamina. $[P^c]$ and $[M^c]$ are the applied cyclic loads and moments. The corresponding cyclic strains of the midplane and curvature $[\epsilon_0^c]$, $[\kappa^c]$ are calculated by inversion of the matrix equation, Eq. (6) to yield

$$[\epsilon_0^c] = [A^{-1}][P^c] - [A^{-1}][B][\kappa^c] \qquad (8)$$

The strain in a particular lamina is given by:

$$_p[\epsilon^c] = [\epsilon_0^c] + {}_pZ[\kappa^c] \qquad (9)$$

The corresponding stresses in the lamina are:

$$_p[\sigma^c] = {}_p[Q][\epsilon_0^c] + {}_pZ_p[Q][\kappa^c] \qquad (10)$$

They are transformed to the lamina principal axes to give σ_A^c, σ_T^c, τ^c, and substituted in the fatigue failure criteria, Eqs. (2) and (3), to predict the first lamina failure.

When only membrane loads exist and the laminate consists of many layers, or the layers are symmetrical about the midplane, then the stiffess matrix $[B]=0$ and Eq. (6) reduce to

$$[\epsilon_0^c] = [A^{-1}][P^c] \qquad (11a)$$

and Eq. (10) reduces to

$$_p[\sigma^c] = {}_p[Q][\epsilon_0^c] \qquad (11b)$$

If, in addition, for any $+\theta$ layer there exists a $-\theta$ layer, then $A_{16} = A_{26} = 0$.

Consider the case when only one normal component of the membrane load exists, say P_x^c (Fig. 1). Then, from Eqs. (11), the applied stresses in each lamina ${}_p\sigma_x^c, {}_p\sigma_y^c$, and ${}_p\tau_{xy}^c$ are found. The transformed stresses in the principal coordinates of the lamina could be expressed as functions of the normal stress alone, similar to that shown in Ref. 2. Thus,

$$_p\sigma_A^c = {}_pk_{xx}\,{}_p\sigma_x^c \qquad (12a)$$

$$_p\sigma_T^c = {}_pk_{yy}\,{}_p\sigma_x^c \qquad (12b)$$

$$_p\tau^c = {}_pk_{xy}\,{}_p\sigma_x^c \qquad (12c)$$

where

$$_pk_{xx} = \frac{1}{2}\left\{\left[1 + \sec 2\theta - \frac{(\mu + \sec 2\theta)\tan^2 2\theta}{\eta + \tan^2 2\theta}\right] + \left[1 - \csc 2\theta - \frac{(\mu - \csc 2\theta)\tan^2 2\theta}{\eta + \tan^2 2\theta}\right]\frac{{}_p\nu_{xy} - \nu_{xy\ell}}{{}_pQ_{xx}/{}_pQ_{yy} - {}_p\nu_{xy}\nu_{xy\ell}}\right\} \qquad (13a)$$

$$_pk_{yy} = \frac{1}{2}\left\{\left[1 - \sec 2\theta + \frac{(\mu + \sec 2\theta)\tan^2 2\theta}{\eta + \tan^2 2\theta}\right] + \left[1 + \csc 2\theta + \frac{(\mu - \csc 2\theta)\tan^2 \theta}{\eta + \tan^2 2\theta}\right]\frac{{}_p\nu_{xy} - \nu_{xy\ell}}{{}_pQ_{xx}/{}_pQ_{yy} - {}_p\nu_{xy}\nu_{xy\ell}}\right\} \qquad (13b)$$

$$_pk_{xy} = -\frac{1}{2}\left\{\frac{(\mu + \sec 2\theta)\tan 2\theta}{\eta + \tan^2 2\theta} - \left[\frac{(\mu - \csc 2\theta)\tan 2\theta}{\eta + \tan^2 2\theta}\right]\frac{{}_p\nu_{xy} - \nu_{xy\ell}}{{}_pQ_{xx}/{}_pQ_{yy} - {}_p\nu_{xy}\nu_{xy\ell}}\right\} \qquad (13c)$$

$$\mu = \frac{1 - E_A/E_T}{1 + 2\nu_A + E_A/E_T} \qquad (14a)$$

$$\eta = \frac{E_A/G_A}{1 + 2\nu_A + E_A/E_T} \qquad (14b)$$

and θ is the angle between the load and the fiber direction (Fig. 1).

Failure of any lamina due to the cycling stress ${}_p\sigma_x^c$ will occur when

$$_p\sigma_x^c \geqq {}_p\sigma_x^u = {}_p\sigma_x^s({}_p\theta) f(R,N,c,\theta) \qquad (15)$$

For the fiber failure mode, it was shown[2] that the fatigue function is independent of the angle ${}_p\theta$; thus failure is expressed by:

$$_p\sigma_x^c \geqq {}_p\sigma_x^u = (\sigma_A^s/{}_pk_{xx}) f_A(R,N,c) \qquad (16)$$

where f_A is the fatigue function of the fiber failure mode as determined from the S – N curve of uniaxial lamina loaded in the fiber direction.

For matrix failure mode, the condition is:

$$_p\sigma_x^c \geqq {}_p\sigma_x^u = {}_p\sigma_x^s f_m(R,N,c,\theta) \qquad (17)$$

where the fatigue function f_m is shown[2] to be:

$$f_m = (R,N,c,\theta) = f_\tau\left[\frac{1 + (\tau^s/\sigma_T^s)^2(k_{yy}/k_{xy})^2}{1 + (\tau^s/\sigma_T^s)^2(k_{yy}/k_{xy})^2(f_\tau/f_T)^2}\right]^{1/2} \qquad (18)$$

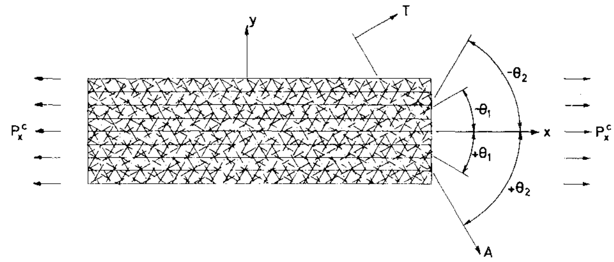

Fig. 1 Coordinates of balanced symmetric laminate.

The static failure (first crack) is expressed by:

$$ {}_p\sigma_x^s = \left[\left(\frac{k_{yy}}{\sigma_T^s}\right)^2 + \left(\frac{k_{xy}}{\tau^s}\right)^2\right]^{-1/2} \tag{19} $$

Substituting for Eq. (17) yields the fatigue failure conditions for first crack:

$$ {}_p\sigma_x^c \geq {}_p\sigma_x^u = \left[\left(\frac{k_{yy}}{\sigma_T^s f_T}\right)^2 + \left(\frac{k_{xy}}{\tau^s f_\tau}\right)^2\right]^{-1/2} \tag{20} $$

Delamination fatigue failure mode is expressed by Eqs. (4) and (5). It was shown in Ref. 3 that the maximum static interlaminar shear stress for angle-ply laminate occurs on the free edge and is expressed by:

$$ \tau_d = \epsilon_{0_x} \frac{2G}{t_i\sqrt{\rho_i}} \frac{Q_{26}Q_{12} - Q_{22}Q_{16}}{Q_{22}Q_{66} - Q_{26}^2} \tanh\sqrt{\rho_i}\,b \tag{21} $$

where

$$ \rho_i = \frac{2G}{t_i t} \frac{Q_{22}}{Q_{22}Q_{66} - Q_{26}^2} $$

For oscillating load, $\epsilon_{0_x} \equiv \epsilon_{0_x}^c$ and $\tau_d \equiv \tau_d^c$. This stress is to be substituted in the criterion, Eq. (4), for predicting fatigue delamination.

Since the interlaminar layer is of the matrix material, it is to be checked whether the shear strength and the interlaminar shear strength are the same; that is,

$$ \tau_d^s \overset{?}{=} \tau^s \tag{22a} $$

$$ f_d(R,N,c) \overset{?}{=} f_\tau(R,N,c) \tag{22b} $$

In order to determine when fatigue failure occurs, it is necessary to apply the failure criteria, Eqs. (1, 3, and 4), for the appropriate number of cycles. In many cases, it would be enough to check for the static failure mode in order to decide which of the fatigue criteria is to be used. For symmetric laminates under certain load conditions, more easily calculated expressions of the failure criteria, such as Eqs. (16) and (17) or (20) and (22) can be used.

When the first lamina fails, the load carried by it transfers to the other laminae.[11] One of two things can happen:

1) The additional load could cause immediate failure of the other laminae and total failure of the laminate. In this case, the first lamina failure is the failure of the laminate and the fatigue failure criteria, as just expressed, are sufficient to predict it.

2) The remaining laminae sustain the new load. In this case, the load on each lamina is raised to a new level. In such cases, the fatigue failure functions are no longer applicable in the preceding form. However, it is possible to use them with the aid of a cumulative damage theory.

The simplest and oldest cumulative damage theory is called Miner-Palmgren rule[8] and is expressed as follows:

$$ (n_1/N_1) + (n_2/N_2) + \ldots = 1 \tag{23} $$

This rule states that at each load level the fraction of damage induced in the material is equal to the fraction of the number of load cycles imposed to the number of load cycles which would have caused failure. When unity is achieved, the material fails. In our case, damage is accumulated in the laminae up to the first lamina failure at some load level, and then damage continues to accumulate after the load redistribution at a higher load level, and so on, until the final fracture.

A more sophisticated cumulative damage theory was presented by Hashin and Rotem.[9] Here, failure is predicted by examining the remaining lifetime after certain load history. Each lamina failure is a movement on a damage curve to the next level on the damage plane of each lamina in the laminate up to crossing the failure curve which indicates failure of the specific lamina. Total failure occurs as before, when the remaining laminae cannot sustain the load.

Experimental

An experimental program was planned and executed in order to verify the analytical concepts of the fatigue failure. A symmetric balanced laminate was chosen as representative of multidirectional laminate. Tension-tension fatigue loading was imposed on a variety of laminates loaded in the symmetrical axes. A failure of a specimen was indicated by a point on an S-N plane to give an S-N curve. These curves were compared with the theoretical predictions. Observation of the failure modes were noted and compared with the expected ones.

Material and Specimen

The fatigue specimens were made of six layers of unidirectional laminae to give a symmetric, balanced laminate. Two layers were in the load direction or perpendicular to it and the other four were in an $\pm\theta$ orientation. A variety of lamination sequences were examined; e.g., the layers in the load direction were in the middle in some specimens, in the outer layers in others, and in the rest, in-between.

The laminate was manufactured in two ways. One was by direct filament winding, where a single end roving of E-glass fibers (Gevatex ES 13 3200XL K921) ran through a bath of epoxy resin (Union Carbide ERL 2256/ZZL0854, 100:31) and was wound on a flat polygonal mandril. The polygon geometry determines the lamination angle. Six thin unidirectional layers were layed up in the sequence desired to produce a balanced laminate. The laminate was put into a vacuum to remove air bubbles and was then cured by heating and pressure. The laminates were then removed from the mandril and cut by a diamond wheel to the desired dimensions.

In the second method, the first steps are the same, but the winding is not on a polygon but on a large diameter drum and is only of one layer. This layer is taken off the drum in the B-stage of polymerization, cut with special tools in the proper angles to fit in a rectangular metal box. Layers are put in the desired orientation, covered with a bleeding plate and put into a vacuum and then cured by heating and pressure. Aluminum tabs were glued to the specimen for proper gripping. The gage length was 100 mm and the cross section 12.7 × 1.5 mm.

The fiber volume fraction in the laminates was 65%. Laminates with the following angles were produced: $[\pm 15, 0\ \text{deg}]_s$ $[\pm 30, 0\ \text{deg}]_s$ $[\pm 45, 0\ \text{deg}]_s$ $[\pm 60, 0\ \text{deg}]_s$ $[\pm 30, 90\ \text{deg}]_s$ $[\pm 45, 90\ \text{deg}]_s$.

Apparatus

Two types of fatigue machines were used for the experiments. Both are of tension-tension type and have an eccentric cam which actuates one of the specimen grips by means of a lever. The first has a very stiff lever, so that one specimen grip attached to it is moving in a sinusoidal pattern. The other grip is attached to a very stiff load cell, thus

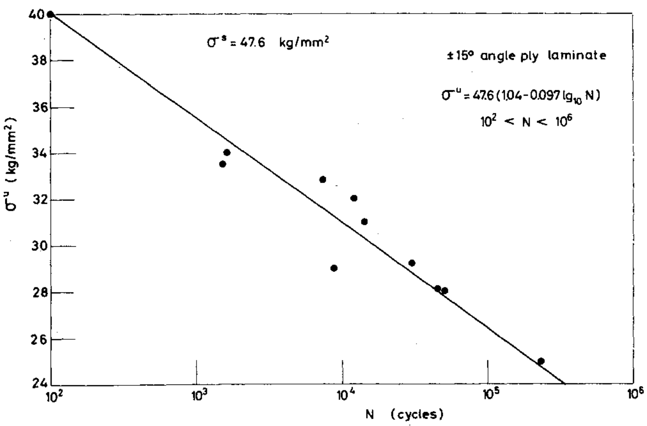

Fig. 2 Fatigue test results of ± 15 deg angle-ply laminate.

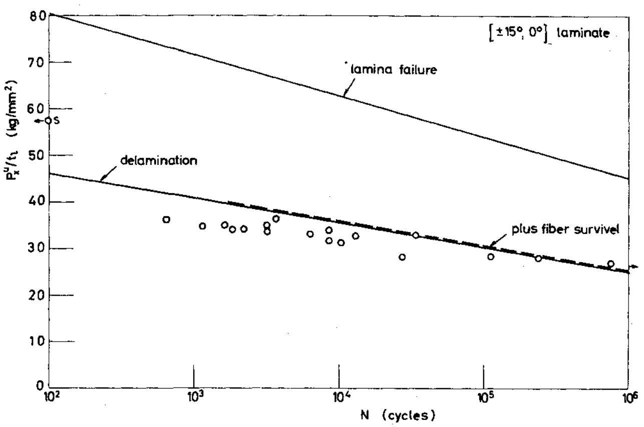

Fig. 3 Test results and predicted S-N curve for [±15, 0 deg] laminates.

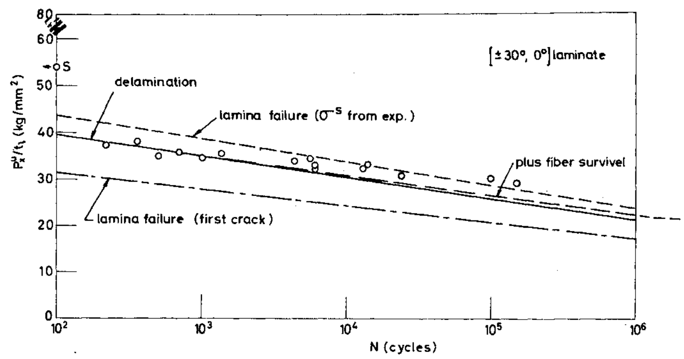

Fig. 4 Test results and predicted S-N curve for [±30, 0 deg] laminates.

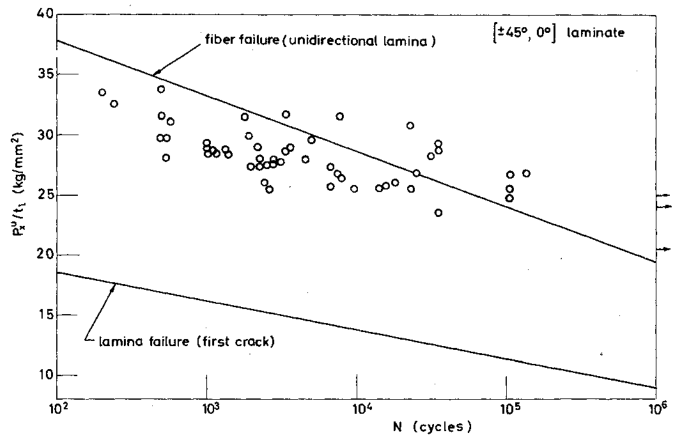

Fig. 5 Test results and predicted S-N curve for [±45, 0 deg] laminates.

producing constant repeated elongation amplitude. The load variation is recorded by the load cell. When some of the laminae failed, a drop in the load was observed but the load on the remaining laminae was almost unchanged. Complete failure was indicated by dropping of the load to near zero.

The second machine was a spring-type lever which connects the cam movement to the grip. As the spring constant is low, there is almost no change in the load applied on the specimen due to permanent elongation during cycling. Thus, this machine performs a constant load amplitude cycling.

Experimental Procedure

The various types of specimens were mounted on the two fatigue machines and their fatigue lives under different stress levels were measured, up to 10^6 cycles. All tests were performed with amplitude ratios of $R=0.1$. Two rates of cycling were used—$c=19$ cycles/s and $c=1.9$ cycles/s. The tests were carried out on both machines for constant elongation amplitude and constant load amplitude. Change of load was recorded on a strip chart recorder. Visual inspection of the failure mechanism was carried out for some specimens.

The material parameters of single lamina needed for the theory are elastic properties, static failure stresses, and the fatigue functions. The first were measured by strain gages and the second with an Instron machine. The lamina fatigue functions have been previously determined in Ref. 1 from the measurements on off-axis specimens, and were used to calculate the fatigue life of angle-ply laminate in Ref. 2. It is recalled that the epoxy used in Ref. 2 and in the present specimens was slightly different from the one used in Ref. 1 (the manufacturer discontinued the previously used epoxy).

The data obtained are given below for E-glass laminate:

$$E_A = 5580 \text{ kg/mm}^2, \quad E_T = 1810 \text{ kg/mm}^2,$$

$$G_A = 613 \text{ kg/mm}^2, \quad \nu_A = 0.285$$

$$\left.\begin{array}{l} f_\tau = 0.917 - 0.0852 \log_{10} N \\ f_T = 0.956 - 0.0541 \log_{10} N \end{array}\right\} 10^2 < N < 10^6$$

$$f_A = 1.123 - 0.11 \log_{10} N$$

$$\sigma_T^s = 4.2 \text{ kg/mm}^2, \quad \tau^s = 8.4 \text{ kg/mm}^2, \quad \sigma_A^s = 126 \text{ kg/mm}^2$$

Results and Discussion

Experimental fatigue failure results for E-glass epoxy laminates were compared with theoretical predictions based on the preceding formulation. The first step in the prediction is to analyze the imposed loading. There are two major categories: elongation amplitude and load amplitude. In the first category, the prediction of the fatigue life should be done separately for each lamina. Failure in a lamina means a crack running parallel to the fibers and the possible inability of the lamina to carry load. However, if the crack does not run to other laminae, there is no total failure. Therefore, total failure is indicated by the longest surviving lamina. From Eq. (2) and the data for the E-glass epoxy, for the 0 deg lamina, we have:

$$\log_{10} N = (141.5 - \sigma_A^u)/13.9 \qquad 10^2 < N < 10^6$$

where σ_A^u is the stress in the unidirectional laminae.

For the $\pm\theta$ deg laminae, Eqs. (17) and (18) or (20) are used to give the number of cycles to failure. For example, the number of cycles to failure of ± 45 deg laminae can be approximated by

$$\log_{10}N = (10 - {}_p\sigma_x^u)/0.7275 \qquad 10^2 < N < 10^6$$

The stress in the laminae is calculated as shown in the Appendix and is substituted in these expressions to give the number of cycles to failure. Delamination is expressed by Eqs. (5) and (21) where the fatigue function f_d is determined from a series of tests on ±15 deg angle-ply laminates, as shown in Fig. 2, to give:

$$f_d = 1.04 - 0.097\log_{10}N \qquad 10^2 < N < 10^6$$

$$\tau_d^S = 12.8 \text{ kg/mm}^2$$

Comparison of these results with the shear fatigue function f_τ shows a very close correlation, which suggests that the matrix materials under fatigue conditions behaves in a similar manner for shear between layers or between fibers, and that tension between laminae is small.

When delamination occurs, it starts at a free edge, propagates inward and is detected by change of the specimen's color. The angle-ply laminae separate from each other and continue to carry a load suitable to the existing strain, as single off-axis lamina. The load carried by the laminate is degraded and laminae fail until the final failure when the last lamina fails.

For load amplitude cycling, the prediction routine is slightly different. Again, the number of cycles to failure is calculated for the different laminae and delamination. However, after the lowest one has been reached, redistribution of the load is calculated and checked for immediate failure of the remaining laminae or for continued cycling under a higher level of loading. The prediction is then for two stages of load level, according to Ref. 9:

$$\left(\frac{n_1}{N_1}\right)^{\frac{1-s_2}{1-s_1}} + \frac{n_2}{N_2} = 1$$

where $s_1 = \sigma_1/\sigma^S$ and $s_2 = \sigma_2/\sigma^S$, σ_1 = the load level in the beginning, σ_2 = the load level after redistribution, n_1 = the number of cycles in load level σ_1, N_1 = the number of cycles to failure in load level σ_1, n_2 = the number of cycles in load level σ_2, and N_2 = the number of cycles to failure in load level σ_2.

The number of cycles to failure would be $n_1 + n_2$. (Usually there are no more than two stages, but sometimes there could be another stage when total failure has not been reached by the second failure, and another redistribution of load takes place.) The different failure modes are calculated separately for the laminate, i.e., delamination, in laminae failure or fiber fracture. The lowest stress failure for a certain number of cycles indicates the onset of the particular failure mode.

Figures 3 and 4 show the experimental results for catastrophic failure and predictions for symmetric-balanced laminates [±15, 0 deg] and [±30, 0 deg] under constant amplitude of load cycling. It is seen that the predicted lamina failures (in the angle-ply laminae) fall much higher than the experimental results. The delamination failure mode is in good agreement with the experimental results and is reinforced by the observation that the specimens indeed fail by delamination. Once delamination occurs, the load on the single off-axis laminae is above their ability to sustain and they crack (see the Appendix for values). The remaining undirectional laminae do not stand up too long either. For load levels above 40 kg/mm^2 they fail immediately. For lower load levels down to 22 kg/mm^2 they survive for some time as shown in Fig. 3 by the dashed line, which is the result of the cumulative damage calculation. For loads under 22 kg/mm^2, there is no fatigue failure of the unidirectional lamina (the possibility of delamination mode has not been tested for cycling over 10^6 cycles).

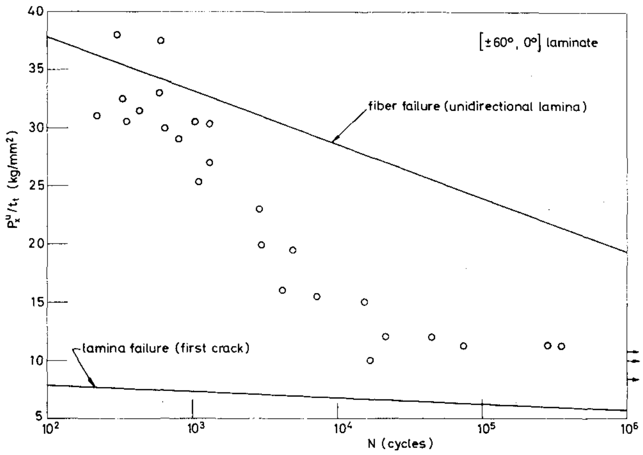

Fig. 6 Test results and predicted S-N curve for [±60, 0 deg] laminates.

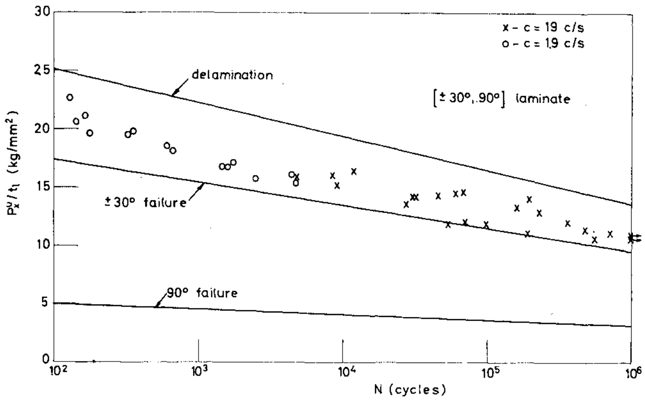

Fig. 7 Test results and predicted S-N curve for [±30, 90 deg] laminates.

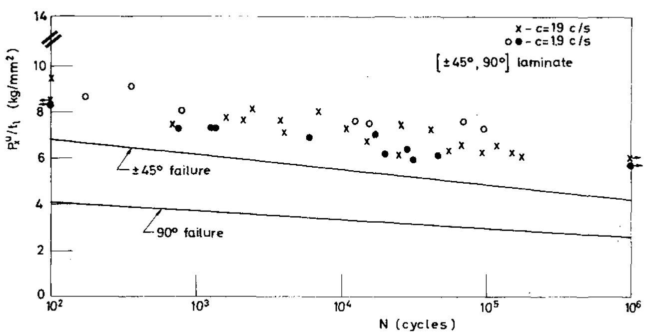

Fig. 8 Test results and predicted S-N curve for [±45, 90 deg] laminates.

Figure 4 shows the experimental results, as well as the predictions for [±30, 0 deg] laminate. It is seen that both delamination and lamina failure modes are close to the test results. Observations show both modes of failure present in a failed specimen and during the experiment. It is seen that the predictions of the onset of lamina failure are at lower stress levels, but when the fatigue failure mode is calculated on the experimental static failure mode[10] (that is, the stress when the lamina fails completely), it gives values higher than the delamination failure mode. Again, the unidirectional laminae survive for an additional short period. The predictions are in good agreement with the experimental results for catastrophic failure.

In Fig. 5, the results of [±45, 0 deg] laminate are given. Delamination cannot occur as the interlaminar shear stress is very low (values are given in the Appendix). The predicted

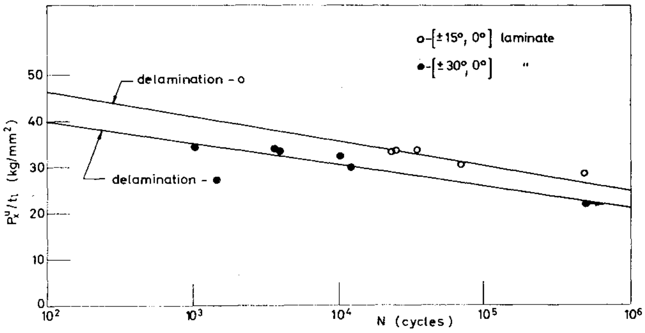

Fig. 9 Test results of constant elongation amplitude tests; dots represent failure of the first lamina, lines represent the predicted failure.

Table 1 Fatigue strength degradation and residual strength

Specimen	P_x^c/t_ℓ Start kg/mm²	P_x^c/t_ℓ End kg/mm²	P_x^s/t_ℓ Remain kg/mm²	N cycles	σ_x 0 deg Remain kg/mm²
±15, 0 deg					
A-1	33.6	11.85	23.7	549000	71.1
A-2	28.6	10.6	30.1	1000000	90.3
A-3	30.5	13.9	37.4	624000	112.2
A-4	33.8	11.3	26.3	502000	89.9
A-5	33.7	13.5	30.7	500000	92.1
±30, 0 deg					
h-1	30.0	17.8	24.2	580000	72.6
h-2	32.4	19.4	27.4	563000	82.2
h-3	22.2	16.8	44.1	500000	132.3

lamina failure gives a low stress level, but because of the spreading of the cracks in the lamina, the laminate remains intact (see Ref. 10) and the total failure is governed by fiber failure of the unidirectional laminae. Hence, this mode is in good agreement with the experimental results for total failure.

In Fig. 6, the results of [±60, 0 deg] laminate are shown, as well as the predictions. As for the [±45, 0 deg] laminate, the lamina failure is the dominant mode, and it causes transfer of the load to the unidirectional laminae. However, it is seen that the fiber failure mode gives overestimated values, unlike in the previous case. The difference is in the total failure of the angle-ply laminae. Here the cracks nucleate in one zone and do not spread as in the ±45 deg laminate (see Ref. 10). This leads to a neat fracture in the angle-ply laminae causing stress concentration in the unidirectional laminae which results in a lower fatigue strength level than the prediction for unidirectional laminae.

Figure 7 shows the results of [±30, 90 deg] laminate. With this laminate, although there is a considerable amount of interlaminar shear stress between the ±30 deg layers, delamination is not expected, as shown by the high value of the imposed load needed for it. In fact, the perpendicular layers start to fail at a very low stress level, but the ±30 deg laminae are the dominant carrying load. It is seen from the figure that prediction of the laminate failure, based on the failure of the ±30 deg laminae, agrees very well with the experimental results for total failure.

Figure 8 shows the experimental results of [±45, 90 deg] laminate. Delamination is not expected in this laminate because of the very low interlaminar shear stress which develop during the tension cycling. Cracking of the 90 deg laminae is predicted at very low stress levels so that here, as in the previous case, the dominant failure mode is expected to be the cracking of the ±45 deg laminae. It is seen from the figure that the prediction is somewhat conservative compared to the experimental results for total failure. This is probably due to the fact that the difference between the 90 deg layers cracking and the ±45 deg layers is not much, so that the perpendicular layers, although cracked in part, carry some of the external load thus raise the strength of the laminate.[11]

The fatigue behavior of the laminates under constant amplitude of elongation cycling is different. Until the first failure, the experimental results, i.e., the S-N curves, are the same as for load cycling. This is due to the almost elastic behavior of the laminate. But, after the first failure of some laminae or delamination, there is no redistribution of loads. Each lamina continues to elongate under the same strain value and thus, the unfailed laminae continue to sustain the same load. Therefore, since the specimens tested did not fail completely, degradation in the applied load was measured.

Figure 9 shows the experimental results of [±15, 0 deg] and [±30, 0 deg] laminates. The dots represent delamination and degradation of load. None of these specimens failed completely under the fatigue loading. The remaining load (when the experiment was stopped) and the remaining strength (measured by tension to failure) are given in Table 1. It seems that up to delamination, behavior is the same as for load cycling, but after delamination, the unidirectional laminae continue to carry the same load and therefore do not fail. There is degradation only in strength due to the cycling, as seen from Table 1. Specimen H-3, which did not suffer from delamination, does not show degradation of strength because of the low stress on the unidirectional laminae when cycling.

Conclusions

The theory of fatigue failure of laminates is based on fundamental fatigue functions connected to the failure criteria. When it is possible to describe the static strength of the laminated composite material using a few values characteristic of the specific material, such as σ_A^S, σ_T^S, τ^S, τ_d^S, which can be measured easily on single lamina and one angle-ply laminate, then the fatigue behavior can be predicted by measuring the corresponding fatigue function and substituting it in the strength criteria. By using these few experimentally measured fatigue functions, and with the aid of the laminate theory, it is possible to predict the fatigue life of many laminates. It is shown that the theory agrees quite well with the experimental results of various laminates, even though the fatigue functions used were rough approximations of the measured ones.

Appendix

The stress field in the laminae of the symmetric-balanced laminate subjected to uniaxial cycling load is calculated as follows:

From Eq. (11a) the strain in the laminate is given by:

$$\epsilon_{0_{xx}}^c = A_{xx}^{-1} P_x^c = \frac{A_{yy}}{A_{xx}A_{yy} - A_{xy}^2} P_x^c = S_{xx_\ell} \frac{P_x^c}{t_\ell} = \frac{P_x^c}{E_{xx_\ell} t_\ell}$$

$$\epsilon_0^c = A_{xy}^{-1} P_x^c = \frac{-A_{xy}}{A_{xx}A_{yy} - A_{xy}^2} P_x^c = S_{xy_\ell} \frac{P_x^c}{t_\ell} = \frac{-\nu_{xy_\ell} P_x^c}{E_{xx_\ell} t_\ell}$$

Assuming the strain is homogeneous throughout the laminate,

$${}_p\sigma_x = {}_pQ_{xx}\epsilon_{0_{xx}}^c + {}_pQ_{xy}\epsilon_{0_{yy}}^c$$

$${}_p\sigma_x = \frac{P_x^c}{A_{xx}A_{yy} - A_{xy}^2} \left({}_pQ_{xx}A_{yy} - {}_pQ_{xy}A_{xy}\right)$$

$${}_p\sigma_x = \frac{P_x^c}{E_{xx_\ell} t_\ell} \left({}_pQ_{xx} - \nu_{xy_\ell}\,{}_pQ_{xy}\right)$$

The extension modulus of the laminate is calculated by:

$$E_{xx_\ell} = \frac{1}{S_{xx_\ell}} = \frac{1}{\Sigma t} \left[\frac{A_{xx}A_{yy} - A_{xy}^2}{A_{yy}}\right]$$

Table A-1 Values for symmetric balanced laminate

Laminate	$[\pm 15, 0\ \text{deg}]_s$	$[\pm 30, 0\ \text{deg}]_s$	$[\pm 45, 0\ \text{deg}]_s$	$[\pm 60, 0\ \text{deg}]_s$	$[\pm 75, 0\ \text{deg}]_s$	$[\pm 90, 0\ \text{deg}]_s$
$\nu_{xy\ell}$	0.3759	0.5212	0.4897	0.3165	0.1708	0.1193
${}_pE_{xx}$(in θ lamina)[a]	3936.1	2369.4	1769.2	1642.9	1732.1	1810.0
$E_{xx\ell}$[a]	5125.1	4033.9	3168.2	2956.3	3014.8	3066.7
${}_\theta\sigma_x/(P_x/t_\ell)$	0.9603	0.8239	0.6366	0.5590	0.5745	0.5902
${}_0\sigma_x/(P_x/t_\ell)$	1.0794	1.3522	1.7270	1.8818	1.8509	1.8195
$K=\tau_d/\epsilon_{0x}$ Eq. (21)[a]	−1052	−937.8	−390.3	+19.07	126.0	0
$\tau_d/(P_x/t_\ell)$	−0.2053	−0.2325	−0.1232	+0.0065	0.0418	0
P_x^s/t_ℓ (experiment)[a]	57.6	54.0	47.3	51.5		
(delam.) P_x^s/t_ℓ (predicted)[a]	62.3	55.0	103.9	1984	306.3	∞
(in-plane) P_x^s/t_ℓ (predicted)[a]	92.8	42.1	18.6	9.57	7.64	7.17
(fibers) P_x^s/t_ℓ (predicted)[a]	101.6	77.1	49.6	48.4	47.1	46.8

[a] Units are kilograms per square milimeter.

and the Poisson ratio:

$$\nu_{xy_\ell}=A_{xy}/A_{yy}$$

The values for symmetric-balanced laminate with equal thickness laminae, two in the 0 deg direction and four in the indicating angles made of E-glass/epoxy, are given in Table A-1.

Acknowledgment

The research reported herein has been supported in part by a grant from the United States-Israel Binational Science Foundation (BSF), Jerusalem, Israel. This support is highly appreciated.

References

[1] Hashin, Z. and Rotem, A., "A Fatigue Failure Criterion for Fiber Reinforced Materials," *Journal of Composite Materials*, Vol. 7, Oct. 1973, pp. 448-464.

[2] Rotem, A. and Hashin, Z., "Fatigue Failure of Angle Ply Laminates," *AIAA Journal*, Vol. 14, July 1976, pp. 868-872.

[3] Puppo, A. H. and Evensen, H. A., "Interlaminar Shear in Laminated Composites Under Generalized Plane Stress," *Journal of Composite Materials*, Vol. 4, April 1970, pp. 204-220.

[4] Pipes, R. B. and Pagano, N. J., "Interlaminar Stresses in Composite Laminates—An Approximate Elasticity Solution," *Journal of Applied Mechanics*, Vol. 41, Sept. 1974, pp. 668-672.

[5] Rybicki, E. F., "Approximate Three-Dimensional Solution for Symmetric Laminates Under Inplane Loading," *Journal of Composite Materials*, Vol. 5, July 1971, pp. 354-360.

[6] Oplinger, D. W., Parker, B. S., and Chiang, F. P., "Edge Effect Studies in Fiber-Reinforced Laminates," AMMRC Tech. Rept. 73-41, Sept. 1973.

[7] Ashton, J. E. and Whitney, J. M., "Theory of Laminated Plates," Technomic Publishing Co., Stamford, Conn., 1970.

[8] Palmgren, A. Z., "Die lebensdauer von Kugellagern," *Z. Ver Deutsch. Ing.*, Vol. 68, 1924, p. 339; Miner, M. A., "Cumulative Damage in Fatigue," *Journal of Applied Mechanics*, Vol. 12, 1945, p. A159.

[9] Hashin, Z. and Rotem, A., "A Cumulative Damage Theory of Fatigue Failure," *Materials Science and Engineering*, Vol. 34, July 1978, pp. 147-160.

[10] Rotem, A. and Hashin, Z., "Failure Modes of Angle Ply Laminates," *Journal of Composite Materials*, Vol. 9, April 1975, pp. 191-206.

[11] Chou, S. C., Orringer, O., and Rainey, J. H., "Post-Failure Behavior of Laminates I-No Stress Concentration," *Journal of Composite Materials*, Vol. 10, Oct. 1976, pp. 371-381.